



DAMAGE EVALUATION AND RESIDUAL CAPACITY OF CONCRETE IN DAMAGED RC COLUMNS

A. Malek⁽¹⁾, A. Scott⁽²⁾, S. Pampanin⁽³⁾, G. A. MacRae⁽⁴⁾

⁽¹⁾ Ph.D. candidate, University of Canterbury, amir.malek@pg.canterbury.ac.nz

⁽²⁾ Senior lecturer, University of Canterbury, allan.scott@canterbury.ac.nz

⁽³⁾ Professor, University of Canterbury, stefano.pampanin@canterbury.ac.nz

⁽⁴⁾ Associate professor, University of Canterbury, gregory.macrae@canterbury.ac.nz

Abstract

The crucial need for reliable and practical technique to assess the structural conditions, including the level of damage and also the residual capacity of RC structures after an earthquake, has been highlighted in the recent earthquake events. Taking a decision on, whether a damaged structure should be demolished, repaired or accepted, directly depends on data and information associated with post-event damage evaluation.

An experimental study was conducted to quantitatively evaluate both residual axial capacity and also the degradation of concrete material in previously damaged reinforced concrete (RC) columns. Three RC circular columns, all 500 mm in diameter and 1500 mm in height were caged such that to provide three confinement levels: low, medium and high. The columns were monotonically subjected to compressive force up to failure. All damaged RC columns were then cut into approximately three equal pieces with two cores taken longitudinally from each piece. The first core was prepared and instrumented for compression testing, while the second core was sliced into a number of 25 mm disks for oxygen permeability testing. Results from compression test on cored cylinders showed an average of 35%, 32% and 30% reduction in strain capacity, ultimate strength and elastic modulus of concrete in the damaged specimen, respectively. This demonstrated that adopting undamaged stress-strain behaviors of concrete material for the purpose of assessment in a damaged RC structure leads to overestimating of the capacity.

Complementary investigation into permeability of damaged concrete disks also led to a damage profile through which the intensity and the extent of damage caused by cracking from the applied axial load, was determined at different locations over the height of the RC columns. The extent of damage was revealed to be up to 25% of the height of the column in the case of low and medium-confined column, while for the high-confined column this length increased to 40% of the column's height.

Keywords: Residual capacity; Damage assessment; Concrete; Permeability

1. Introduction

Evaluation of damage and residual capacity of the damaged structures is the first priority after a seismic event. This will let vulnerable structures, which cannot withstand service load and/or further seismic actions, to be identified. Thus, authorities will be provided with a basis to make a decision, as to whether damaged building to be demolished, repaired or even accepted without repair, which is of great importance for the remediation plan. Amongst structural members, columns should be prioritized in the evaluation process since the lack of sufficient capacity to sustain loading demand may cause a progressive collapse of the structure. A key step to estimate the residual capacity of an RC member is to designate appropriate mechanical properties of the concrete material and reinforcing bars. Although the idea of determining residual capacity at the structure or member level has drawn considerable attention from researchers [1-6], it has not yet been broadly studied from a concrete material point of view.

To assess the damage occurred in the concrete material, there is a desperate need to employ appropriate damage detection technique. To date, a vast variety of test methods varying from the simple rebound hammer test [7] to a highly sophisticated technique computational tomography (CT) [8], have been introduced to examine damage occurs in the properties of the concrete material. The structural cracks in concrete induced by external loading are not only indicative of damage, but also allow for a rapid fluid transport, resulting in a higher permeable material. Permeability test which is conventionally used as an indication of durability has been proven capable enough to reveal the potential of microcracks presented in mechanically damaged concrete [9]. The permeability of concrete is recognized as an intrinsic feature which allows fluids to transfer through a porous medium at the presence of pressure gradient. The relationship between permeability and microcracking damage at low-level stress (from 0 to 15% of ultimate strength) has been experimentally investigated by [10]. In the study conducted by Sugiyama et al. [11] on the effect of a compressive stress on the permeability of concrete, it was found that the permeability considerably increases once the stress level exceeds 75% of the ultimate strength of normal concrete. Observations by Hearn and Lok [12] also exhibited a significant increase of air permeability at the critical stress level of 71% of the ultimate axial strength. The application of permeability to assess cracked plain concrete has been studied in the past [13-15]. However, there are limited studies in the literature addressing permeability-based damage evaluation at reinforced concrete member level [16-18].

As the above discussion attests, the oxygen permeability test was employed to determine initially damage in terms of change in the permeability feature of damaged concrete and also its extent with respect to the propagation of cracking in the RC columns. In the complementary phase of the study, an attempt was also made to determine the residual capacity of the concrete material in terms of post-damage stress-strain behaviors. For this, cored cylinders were taken from the confined central area of axially pre-loaded RC columns. The mechanical properties of the damaged concrete material, including elastic modulus, ultimate compressive strength and maximum strain capacity, were precisely measured.

2. Experimental program

2.1 Specimen properties

Three circular RC columns all 1500 mm in height and 500 mm in diameter were constructed. Columns were caged using 12 deformed bars all 16 mm in size for longitudinal bars and also a 12 mm plain bar as a transverse reinforcement. Three different transverse reinforcement configurations were fabricated to represent three confinement conditions: low, medium and high. All three columns were poured with the same concrete batch, provided by a local ready-mix supplier with specified target strength of 40MPa at 28 days, and a slump of 80 mm. The general purpose (GP) cement was used and the aggregate was semi-crushed with a maximum size of 19 mm. To simulate the three different confinement levels, transverse reinforcements with spiral spacing of 40 mm,

70 mm and 105 mm were placed over 1 m at the mid-height of the columns. The transverse reinforcement was placed closer in the upper and lower quarters of the columns to transfer damage to the middle part of each column. The details of column specimens and transverse reinforcement are illustrated in Fig 1.

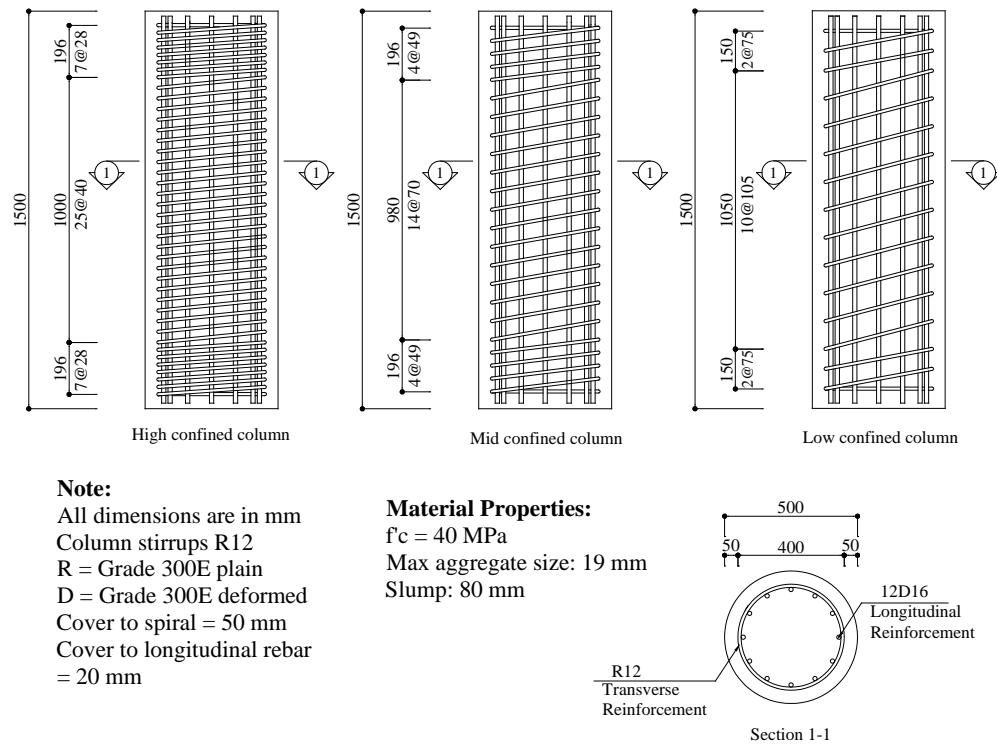


Fig. 1- Details of the column assemblies

2.2 Test protocol

The test apparatus accommodates the column to be loaded axially using the 10,000 kN Dartec Universal Testing Machine. The machine has a fixed reaction at the base extending from floor level and a movable reaction head at top allowing load to be evenly distributed on the test specimen. The experiment conducted in monotonic axial compression displacement rate of 0.1mm/s. Both applied load and overall displacement occurred in the specimens, measured during testing through load cell installed on the machine. The axial deformation on each column was also recorded via 8 linear variable displacement transducers (LVDT), over a central 450 mm gauge length. The appearance of vertical cracks in the cover concrete was the first damage observation as the loading applied to the specimen proceeded. Local crushing and subsequent spalling of the cover concrete stimulated quick propagation of these cracks. In spite of spalling of the cover concrete, which made it malfunction, the presence of spiral reinforcement boosted both ductility and strength features of the remaining concrete core.

For both high and medium confined columns no distinctive failure plane was observed. The vertical cracks were formed in the central part of the columns just after the peak load. The concrete cover of the damaged area was spalled after the peak load. Hoop fracture occurred as a consequence of hoop expansion in the central part of the column. All longitudinal bars were buckled, and concrete located in the core of column was seriously crushed. Fig. 2 shows the ultimate damaged status of the columns at the end of the test. In the case of the low-confined column, a different failure pattern mechanism was observed. The collapse happened by virtue of shear diagonal sliding of the upper and bottom parts of the column, due to the formation of a diagonal failure plane. The propagated cracks in the low-confined column were mainly formed from one-third of the height to the top of the column. Therefore, the concrete cover of approximately one-third of the height of the column remained almost non-damaged. The concrete cover of

the damaged area was spalled after the peak load. After the first hoop fracture, a diagonal failure plane was observed, and all longitudinal bars were buckled.

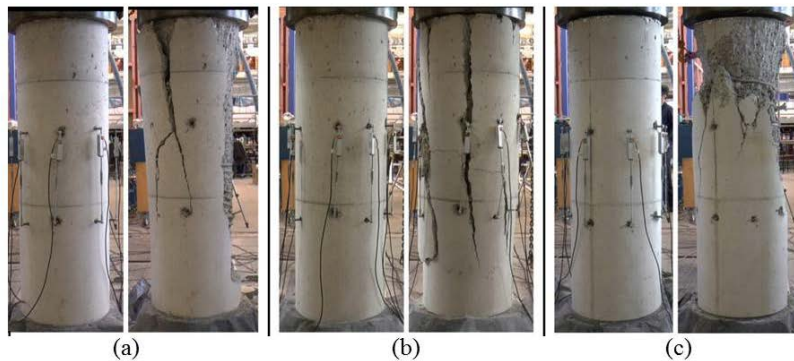


Fig. 2- Failure modes of RC columns (a) High confined (b) Medium confined (c) Low confined

Fig. 3 presents the comparison of the pushdown axial force-axial displacement results for three columns in this study. The axial capacity of test specimens increased by increasing compressive load up to peak, whereupon degradation in strengths was observed. This is mainly due to the buckling of longitudinal bars, yielding and fracture of the spiral reinforcements.

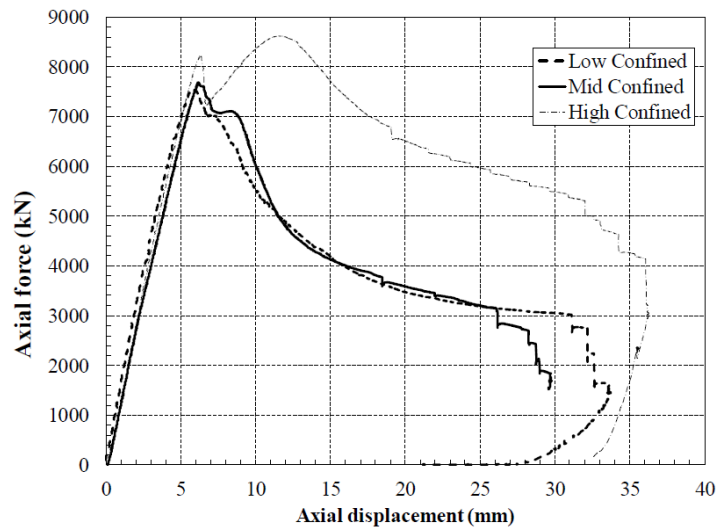


Fig. 3- Force-displacement response of RC columns

3 Damage assessment

To evaluate the level of damage incurred by axial loading on concrete material in a collapsed RC column under monotonic compression force, two approaches were utilized. The first followed the idea of establishing an oxygen permeability coefficient profile over the height of a damaged RC column, while the second attempted to capture the remaining stress-strain capacity of the concrete material. The key step to achieve these goals is to provide some concrete cores drilled from areas of interest in the collapsed columns. The coring procedure was planned to be conducted vertically to avoid cutting any reinforcement, getting cores in the direction that material has been previously loaded and also taking sequential cores as much as possible to come up with a continuous profile. Therefore, damaged RC columns were all laid down and cut into three pieces to enable coring from the

central part of the sections. Fig. 4 shows the cutting procedure and also final cut pieces obtained from the top, medium and bottom parts of each damaged column.

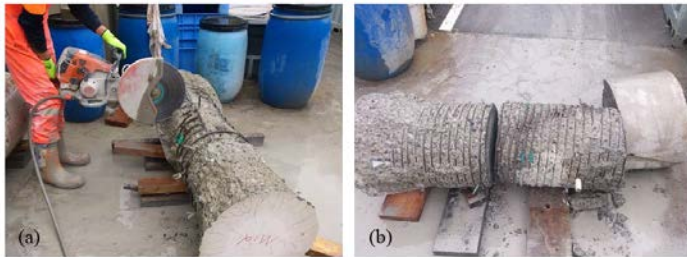


Fig. 4- (a) Cutting process (b) Final cut pieces

A diamond core bit with working length of 430mm and nominal diameter of 93 mm was used along with the core drill machine to take desired cores from the damaged pieces. The location was selected in a way that avoided any facing with embedded reinforcement. Two companion cores were taken from each piece to provide enough material for both permeability and supplementary compression tests. One core was used to supply concrete disks distributed over the height of the column, however, no disks could be obtained in the highly central damaged area of the high-confined column. The second core, was secured for a compression test to capture the stress-strain relationship in the damaged concrete core.

3.1 Oxygen permeability test

To conduct the permeability test, at first, 25mm-thick disks were extracted and appropriately prepared from damaged concrete cores. Slicing began precisely from one end of the core once the uneven portion had been removed and continued until the whole core was used. The disks were completely dried before proceeding to any gas permeability test. Fig. 5a shows the disks were oven-dried at 50°C until the disks reached a steady state moisture content.

A permeability cell was utilised to determine the permeability index [19]. This test set up consists of a constant head permeameter in which oxygen is served as the permeating substance. The cell comprises of inlet and outlet valves which allow oxygen flows through the chamber. The specimens were then placed at the top of the permeability cell, and a pressure head difference up to 100 kPa was applied (Fig. 5b). Permeability measurements were conducted in an air-conditioned room. After initiating the percolation of oxygen through the disks, sufficient time is needed to reach steady state gas flow. The pressure decay of oxygen is recorded by the transducer at five minute time intervals. The test is terminated either after eight hours or a 50 kPa drop in pressure.

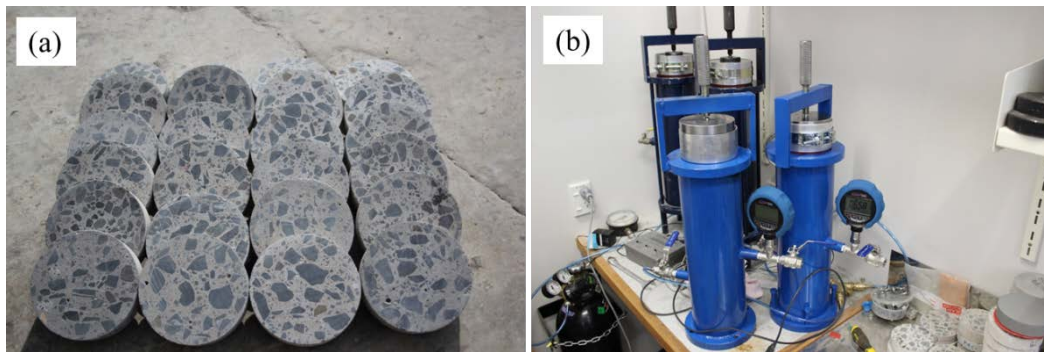


Fig. 5- (a) Concrete disk (b) Oxygen permeability test apparatus

The apparent coefficient of permeability (m/sec) is calculated from the expression of Eq. (1) for laminar flow of a compressible fluid [20].

$$k = \frac{\omega V g d z}{R A \theta} \quad (1)$$

Where ω = molecular mass of oxygen (kg/mol); V = volume of oxygen under pressure (m^3); g = acceleration due to gravity (m/s^2); d = sample thickness (m), z = slope of line $\ln(P_o/P_t)$, R = gas constant, $8.314 (JK^{-1}mol^{-1})$; A = cross-sectional area (m^2); θ = absolute temp ($^{\circ}k$); P_o = Initial pressure reading at the start of the test (kPa); P_t = subsequent pressures during experiment obtained at each step (kPa).

3.2 Quantitative permeability damage evaluation

Having measured the oxygen permeability index (OPI) of all disks taken continuously over the height of the damaged column, the OPI profile can be established. Fig. 6a indicates the variation of coefficient of permeability over the height of the damaged column. This profile provides a basis to spot the location of local damage and also determine how far the damage has spread out with regard to the increase in permeability. These profiles reveal how far it is necessary to move away from the visibly damaged area to assure concrete is essentially undamaged.

As it can be seen, the OPI increased 32 times from an average value of 22×10^{-11} m/sec over the upper and bottom thirds of the column to 700×10^{-11} m/sec as the peak value over the central area for the low-confined column. The OPI of the medium-confined column also surged from an average of 35×10^{-11} m/sec in the relatively lower damaged area in the vicinity of both ends of the column, to 734×10^{-11} m/sec at the extremely damaged zone in the middle part of the column. The OPI associated with the low and medium-confined columns, achieved approximately similar values, which shows that in the areas in which the disks can be taken, confinement did not significantly affect the permeability. In the case of the high-confined column, there was no chance to plot a continuous diagram because of the severe damage which did not allow extracting concrete disks from the extremely damaged zone. The average of OPI in the relatively undamaged area of the high-confined column is 62×10^{-11} m/sec, which is two times bigger than the OPI value related to the same zones in the low and medium-confined columns. If it were possible to measure OPI, it would offer no resistance to flow, resulting in a considerably large off-scale value.

The OPI values calculated for all disks, taken over the height of the columns can also serve to introduce a damage parameter, addressing the material deterioration through change which happens in permeability. Damage parameter, D, can be estimated as a relative change in permeability, as follows:

$$D = \frac{k - k_0}{k_{peak}} \quad (2)$$

Where k = measured coefficient of permeability of the concrete disk at any location; k_{peak} = the coefficient of permeability of the concrete core taken from the highly damaged area, and k_0 = the coefficient of permeability of the concrete core taken from the relatively undamaged area. In practice, it is impossible to get a disk from a highly damaged area, especially in the high-confined column, as the concrete is completely crushed to loose and un-integrated aggregates. The damage parameter is defined as a relative quantity because k_0 is obtained from the cores taken from the most intact areas of the specimen, not from the concrete cylinder prepared during casting. That is because in practice it is very unlikely to have access to these cylinders, thus considering concrete disk samples extracted from relatively undamaged areas makes good sense.

Fig. 6b shows the variation of the damage parameter over the height of the column as a function of permeability. The damage parameter achieves the highest values of 0.99 and 0.98 for low and medium-confined columns, respectively over the central zone, since the middle part is significantly prone to stresses generated during the test. It decreases drastically once it reaches both top and bottom ends which match with observations during the test. For the case of the high-confined column, the graph cannot continuously be plotted over the central zone due to the impossibility of preparing disks from this area. The extent of the damaged area associated with the high-confined column is greater than the others. This

is substantially attributed to the higher level of stress during loading in the region. The extent of damage for low and medium-confined columns was 350 mm, which is 25% of column height, while for the high-confined column this length increases to 600 mm, which is 40% of the height.

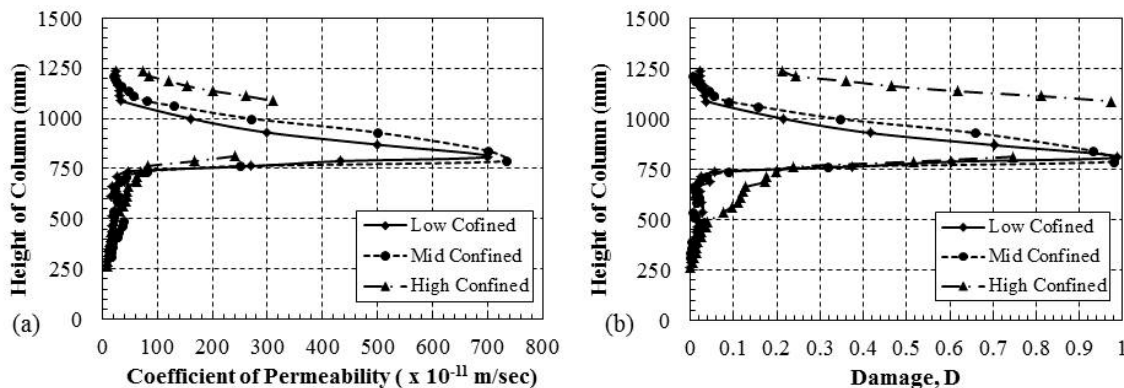


Fig. 6- (a) Permeability profile over the height of the damaged column (b) Damage parameter distribution

4. Residual capacity and material degradation of damaged concrete cores

Once the stress-strain behaviour is established, it would be possible to characterize how the material behaves during loading, where it is supposed to have failed (ultimate strength), and how much strain it can sustain up to failure, suggesting the ultimate ductility. To find out how much capacity has remained in a damaged concrete material, there is a need to determine how much reduction in the ultimate strength and strain (material degradation) has occurred in the specimen with respect to applied damage. For this purpose, concrete cores were cut in a length of approximately 186 mm, to maintain height/diameter ratio of 2, and also to be consistent with the results of intact cylinders. Two PL-60-11 strain gauges (TML Tokyo Sokki Kenkyujo) with a gauge length of 60 mm were axially attached to the prepared surface using cyanoacrylate CN-E adhesive on each core cylinder to measure the axial strain. To account for any asymmetric axial strain inconsistency, strain gauges were mounted at 180° intervals. The circumferential strains were also measured using the same type of strain gauges laid on the mid-height of both sides of each specimen. The samples were then loaded at the rate equal to 400 $\mu\epsilon$ /min using a cyber-plus compression machine of 3000 KN capacity up to failure to determine residual stress-strain capacity of the cylinders.

Residual stress-strain capacity obtained from the compression test on core samples was plotted in Fig. 7. It should be noted that both axial and transverse strain values presented herein are the average readings of two pairs of strain gauges for each sample. The average strain and strength capacity of intact cylinders cured in the fog room, and tested at the age of 180 days, was 2490 $\mu\epsilon$ and 40MPa, respectively. The average of strength and strain of three cores taken from the top, mid and bottom parts of the low-confined column presented an average value of 26 MPa and 1440 $\mu\epsilon$, consecutively. In the low-confined column, the weakest core was taken from the top part, which acquired 1007 $\mu\epsilon$ and 24 Mpa (Fig. 7a). The average of the strength in the cores procured from the column with the medium confinement was 29 MPa, while its strain acquired 1540 $\mu\epsilon$ (Fig. 7b). The least value in this case was related to the core from the middle part, which showed 1320 $\mu\epsilon$ as its strain capacity. In the case of cores taken from the high-confined column, the average of the strain and strength measured from all three cores was 1360 $\mu\epsilon$ and 25 MPa. Similar to the medium-confined column, the minimum of strength and strain values were still associated with the middle part, which showed only a strength of 12 Mpa, and strain equal to 612 $\mu\epsilon$ (Fig. 7c).

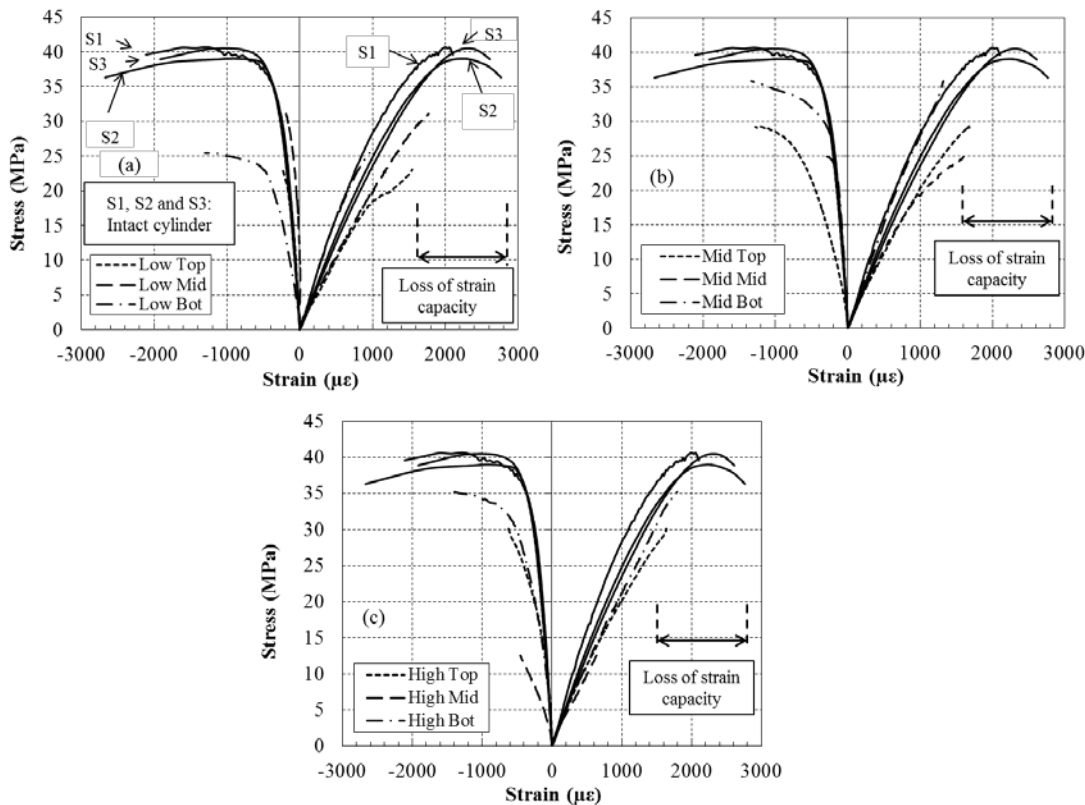


Fig. 7- Residual stress-strain capacity of damaged core (a) low-confined column (b) medium-confined column (c) high-confined column

Having compared the average ultimate strain capacity of intact concrete cylinders with damaged cores in all parts of all three specimens, about $1100 \mu\epsilon$ reduction in the ultimate strain of damaged concrete was observed, which represents 44% loss of strain capacity. Overall, the cores taken from the middle part of the high-confined column presented the least strain capacity. This remaining strain capacity indicated damage, which had occurred in terms of microcracking leading to 75% loss of strain capacity in this type of column. It was also found that the strain capacity of cores taken from the bottom part of all three types of columns is higher than the other segments. With respect to strength capacity, the average of strengths obtained from all cores showed 32% drop in comparison with undamaged cylinders. This study also showed that cores extracted from the middle part of columns with low and medium level of confinement show less strain and strength compared to the cores from the top and bottom parts, which implies this middle area has been more affected by the damage.

Compressive behavior of damaged cored cylinders showed the elastic modulus of damaged concrete is also relatively lower than undamaged concrete. Results show more deviation from the elastic modules of undamaged cylinders once stress increases. The average of the elastic modulus of the three undamaged concrete cylinders, calculated from the axial branch, is 31.3 GPa, while the average of E-modulus between all damaged cores is 21.8 GPa. This is an indication of 30% degradation in stiffness.

5. Conclusion

The purpose of this work was to evaluate damage in the concrete material obtained from RC columns, in an attempt to correlate material degradation and the level of damage. In fact, when the material characterization of an existing concrete building is required, recognition of mechanical properties of the concrete is the first priority in the evaluation process. To achieve this goal, two concerns should be dealt with: applying a robust and reliable technique to assess both the level and the extent of damage that has occurred in the specimen and, secondly,

understanding the amount of loss in strength and strain capacity (material degradation). It was found that the permeability test is reliable enough to correlate observed damage with material degradation. The supplementary investigation conducted to capture stress-strain behaviour also led to the estimation of the residual axial capacity of the damaged concrete material.

Using the profile of permeability over the height of the damaged RC column, the extent of damage was identified, which was in excellent agreement with measured laboratory observations. Once concrete cracked, the permeability typically increased up to 28 times the slightly cracked permeability for the specimens under uniaxial loading. The largest permeability coefficient reported in this study is related to the sample was taken from the mid-height of the column. The extent of damage for low and medium-confined columns was 350 mm, which is 25% of column height, while for the high-confined column this length increases to 600 mm, which is 40% of the height.

The experimental results on partially damaged cores taken from column showed a significant reduction of E-modulus, strain and strength. The study showed E-modulus, strain and strength capacity were all affected by the strain/stress level applied during testing, such that, 35%, 32% and 30% degradation were experienced, consecutively. This could imply that damage (e.g. crushing) would occur earlier if the damaged member was subject to the next loading demand (i.e. earthquake/aftershock). In other words, to determine the residual capacity of a damaged RC member, stress-strain diagrams related to intact concrete are no longer valid and a revised relationship, showing the damaged stress-strain relationship should be used. This also shows that adopting undamaged stress-strain behaviors of concrete material for the purpose of assessment in a damaged RC structure leads to overestimating of the capacity. It was also found that lateral strain is a better indicator of damage since it experienced higher loss compared to axial strain.

6. Acknowledgement

The authors would like to acknowledge the funding provided for the project by the MBIE via the Natural Hazard Research Platform. The assistance of the staff of the structure lab of the University of Canterbury for their support throughout the experimental stage of this study is appreciated.

7. References

- [1] Tasai A (1999): Residual axial capacity and restorability of reinforced concrete columns damaged due to earthquake. *PEER Report, 10*, 191-202, Pacific Earthquake Engineering Research, Berkeley, USA.
- [2] Chung YS, Park CK, Meyer C (2008): Residual seismic performance of reinforced concrete bridge piers after moderate earthquakes. *ACI Structural Journal, 105*(1), 87 –95.
- [3] Maeda M, Kang DE (2009): Post-earthquake damage evaluation for reinforced concrete buildings. *Journal of Advanced Concrete Technology, 7*(3), 327-335.
- [4] Bao X, Li B (2010): Residual strength of blast damaged reinforced concrete columns. *International journal of impact engineering, 37*(3), 295-308.
- [5] Baghaei R, Feng MQ, Torbol M: Residual capacity estimation of bridges using structural health monitoring data. Proc., SPIE Smart Structures and Materials+ Nondestructive Evaluation and Health Monitoring, International Society for Optics and Photonics, 79833I-79833I-79812.
- [6] Li B, Nair A, Kai Q (2012): Residual axial capacity of reinforced concrete columns with simulated blast damage. *Journal of Performance of Constructed Facilities, 26*(3), 287-299.
- [7] Greene GW, (1954): Test hammer provides new method of evaluating hardened concrete. *Proc., ACI Journal Proceedings, 51*(11), 249 –256.
- [8] Landis EN, Nagy EN, Keane DT (2003): Microstructure and fracture in three dimensions. *Engineering Fracture Mechanics, 70*(7), 911-925.

- [9] Picandet V, Khelidj A, Bastian G (2001): Effect of axial compressive damage on gas permeability of ordinary and high-performance concrete. *Cement and Concrete Research*, **31**(11), 1525-1532.
- [10] Choinska M, Khelidj A, Chatzigeorgiou G, Pijaudier-Cabot G (2007): Effects and interactions of temperature and stress-level related damage on permeability of concrete. *Cement and Concrete Research*, **37**(1), 79-88.
- [11] Sugiyama T, Bremner TW, Holm TA (1996): Effect of stress on gas permeability in concrete. *ACI Materials Journal*, **93**(5), 443-450.
- [12] Hearn N, Lok G (1998): Measurement of permeability under uniaxial compression: a test method. *ACI Materials Journal*, **95**(6), 691-694.
- [13] Wang K, Jansen DC, Shah SP, Karr AF (1997): Permeability study of cracked concrete. *Cement and Concrete Research*, **27**(3), 381-393.
- [14] Kermani A (1991): Permeability of stressed concrete: Steady-state method of measuring permeability of hardened concrete studies in relation to the change in structure of concrete under various short-term stress levels. *Building research and information*, **19**(6), 360-366.
- [15] Tegguer AD, Bonnet S, Khelidj A, Baroghel-Bouny V (2013): Effect of uniaxial compressive loading on gas permeability and chloride diffusion coefficient of concrete and their relationship. *Cement and concrete research*, **52**, 131-139.
- [16] Girrens SP, Farrar CR (1991): Experimental assessment of air permeability in a concrete shear wall subjected to simulated seismic loading, Los Alamos National Laboratory.
- [17] Hutchinson TC, Soppe TE (2011): Experimentally measured permeability of uncracked and cracked concrete components. *Journal of Materials in Civil Engineering*, **24**(5), 548-559.
- [18] Soppe TE, Hutchinson TC (2011): Assessment of gas leakage rates through damaged reinforced-concrete walls. *Journal of Materials in Civil Engineering*, **24**(5), 560-567.
- [19] Ballim Y (1991): A low cost falling head permeameter for measuring concrete gas permeability. *Concrete Beton*, **61**, 13-18.
- [20] Alexander M, Ballim Y, Mackechnie J (1999); *Concrete durability index testing manual, Research Monograph No. 4*. Department of Civil Engineering, University of Cape Town.